

Reasons Two Nonstrained C–C σ -Bonds Can Be Easily Cleaved in Decyanative [4 + 2] Cycloaddition Catalyzed by Nickel(0)/Lewis Acid Systems. Theoretical Insight

Wei Guan,^{†,‡} Shigeyoshi Sakaki,^{*,†} Takuya Kurahashi,[§] and Seijiro Matsubara[§]

[†]Fukui Institute for Fundamental Chemistry, Kyoto University, Kyoto 606-8103, Japan

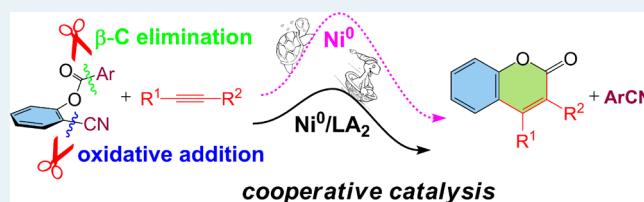
[‡]Faculty of Chemistry, Institute of Functional Material Chemistry, Northeast Normal University, Changchun 130024, People's Republic of China

[§]Department of Material Chemistry, Graduate School of Engineering, Kyoto University, Kyoto 615-8510, Japan

Supporting Information

ABSTRACT: Two nonstrained C–C σ -bonds are cleaved in a novel nickel(0)/LA-catalyzed decyanative [4 + 2] cycloaddition of *o*-arylcarboxybenzonitrile with alkyne, where LA represents a Lewis acid such as methylaluminum bis(2,6-*di*-*tert*-butyl-4-methylphenoxide). The catalytic cycle of this reaction is systematically investigated here by DFT method to clarify the reasons two nonstrained C–C σ -bonds are successfully cleaved in this reaction. DFT calculations indicate that this reaction occurs via the oxidative addition of the C–CN σ -bond of *o*-arylcarboxybenzonitrile to the Ni(0) center, alkyne insertion into the Ni(II)–aryl bond, C–C coupling between the vinyl carbon and the carboxyl carbon atoms, and β -aryl elimination followed by reductive elimination. One LA interacts with the cyano nitrogen atom of *o*-arylcarboxybenzonitrile to accelerate the oxidative addition by stabilizing the unoccupied $\sigma^* + \pi^*$ C–CN antibonding orbital. One more LA interacts with the carbonyl oxygen of *o*-arylcarboxybenzonitrile. This LA enhances the electrophilic nature of the carbonyl carbon to accelerate the C–C coupling, because this step occurs through the nucleophilic attack of the vinyl carbon at the carbonyl carbon atom. The second C–C σ -bond activation occurs via β -aryl elimination, the transition state of which is stabilized by the interaction between LA and the carbonyl oxygen atom. These results lead to the clear conclusion that the presence of two LA molecules is crucial to achieve the dual C–C σ -bond cleavages. The reasons LA accelerates the oxidative addition of the C–CN σ -bond to the nickel(0) center and the C–C coupling followed by the β -aryl elimination are discussed in detail.

KEYWORDS: C–C bond activation, nickel complex, Lewis acid, density functional theory calculation, synergy effect



INTRODUCTION

The selective activation of nonstrained inert C–C σ -bonds has attracted much attention because of its powerful and wide application to organic syntheses and catalytic reactions.¹ This process is not only helpful for the construction of complex molecular skeletons from simple starting materials but also satisfies atom economy.² However, the process still faces tremendous challenges due to the inertness of the nonstrained C–C σ -bond, considering that the C–C σ -bond cleavage is more difficult than C–H σ -bond cleavage because both sp^3 orbitals of two carbon atoms extend well toward each other in the C–C σ -bond and thereby an incoming metal center cannot interact well with these sp^3 orbitals.³ In the past decade, a great deal of effort has been made to develop transition-metal-mediated C–C σ -bond cleavage by utilizing the release of ring-strain energy of the highly strained substrate,⁴ aromatization by C–C σ -bond cleavage,⁵ stabilization by cyclometalation,⁶ and irreversible elimination of functional group(s) such as carboxyl(s),⁷ carbonyl(s),⁸ and cyano(s).⁹

A novel strategy making use of synergistic effects by metal–metal,¹⁰ metal–organic,¹¹ and organic–organic¹² combined

catalysts is now receiving new attention. An efficient cooperation of the transition-metal (TM) complex with the Lewis acid (LA) is expected to be a powerful tool in C–C σ -bond cleavage.¹³ In a series of recent works, it was noted that C–CN σ -bond activation is promoted well by TM/LA cooperative catalysis.^{14–17} Jones and co-workers investigated the kinetics and thermodynamics of competitive C–CN and C–H σ -bond activation reactions in the interconversion of aryl cyanide by Ni(dippe) (dippe = diphenylphosphinoethane) and found that the C–CN σ -bond cleavage of aryl cyanide can be achieved rapidly and exclusively at low temperature in the presence of a LA such as BPh₃.¹⁴ Nakao, Hiyama, and co-workers made outstanding contributions to the application of similar TM/LA cooperative catalysts to the organic syntheses of various organic nitriles.¹⁵ They successively reported that Ni⁰/LA cooperative catalysts are highly effective for the carbocyanation of unactivated alkynes and alkenes via C(sp , sp^2 , and sp^3)–CN σ -bond cleavage. Jacobsen et al. accomplished asymmetric intramolecular arylcyanation of alkenes using chiral

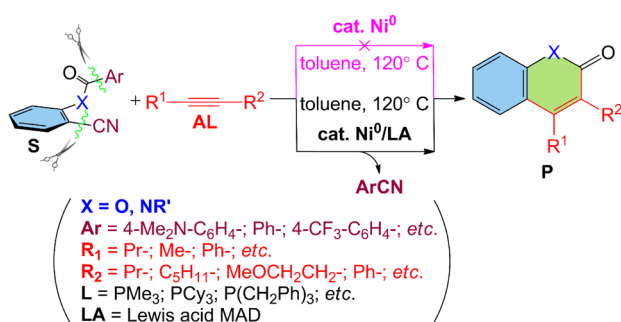
Received: October 26, 2014

Published: November 3, 2014

Ni^0 complexes in the presence of BPh_3 .¹⁶ Nakao, Hiyama, Ogoshi, and co-workers also reported similar reactions catalyzed by a nickel(0) complex and AlMe_2Cl instead of BPh_3 .^{15c} In all of the aforementioned works, LA significantly improves the yield of the product, accelerates the reaction rate, and/or even makes a very difficult reaction possible.

Matsubara, Kurahashi, and co-workers recently developed an unprecedented intermolecular cycloaddition reaction using a Ni^0/MAD catalytic system (MAD = methylaluminum bis(2,6-di-*tert*-butyl-4-methylphenoxide)), where *o*-arylcarboxybenzotrile and *o*-cyanophenylbenzamide react with alkynes to afford coumarins and quinolones, respectively^{18,19} (see Scheme 1). It

Scheme 1. Experimentally Reported Ni^0/LA -Catalyzed Decyanative [4 + 2] Cycloadditions of *o*-Arylcarboxybenzotrile and *o*-Cyanophenylbenzamide with Alkynes^{18,19}



should be noted that this reaction occurs via the cleavage of two nonstrained C–C σ -bonds and that a Lewis acid such as MAD must be added to the reaction system in an amount of 3 molar equiv to the Ni^0 complex. Although theoretical and experimental studies of the C–CN σ -bond cleavage have been carried out for a number of low-valent TM complexes containing Fe,²⁰ Co,²¹ Ni,²² Cu,²³ Mo,²⁴ Ru,²⁵ Rh,²⁶ Pd,²⁷ and Pt,²⁷ the mechanistic details and the origins of cooperative and synergistic functions of the TM/LA catalytic system are not clear at all. Also, the role of LA has not been theoretically investigated in TM-catalyzed C–C σ -bond activation, while the role of LA was theoretically discussed in C–H σ -bond activation²⁸ and Diels–Alder reactions.²⁹ Hence, it is necessary to provide theoretical knowledge of this TM/LA cooperative catalysis for C–C σ -bond cleavage. Such knowledge is indispensable to obtain a good understanding and further develop the activation reaction of the inert C–C σ -bond.

In the present work, we theoretically investigated the full catalytic cycle of the Ni^0/LA -catalyzed [4 + 2] cycloaddition of *o*-arylcarboxybenzotrile with alkyne by density functional theory (DFT). Our purposes here are to clarify the mechanism of this catalytic reaction, compare the catalytic cycle between the absence and the presence of LA, and elucidate the reasons two nonstrained C–C σ -bonds can be successfully cleaved by this catalytic system. We wish to provide a general understanding of how to achieve the nonstrained C–C σ -bond cleavage.

COMPUTATIONAL DETAILS AND MODELS

All geometry optimizations were performed using the M06 functional.³⁰ This hybrid functional was chosen here on the basis

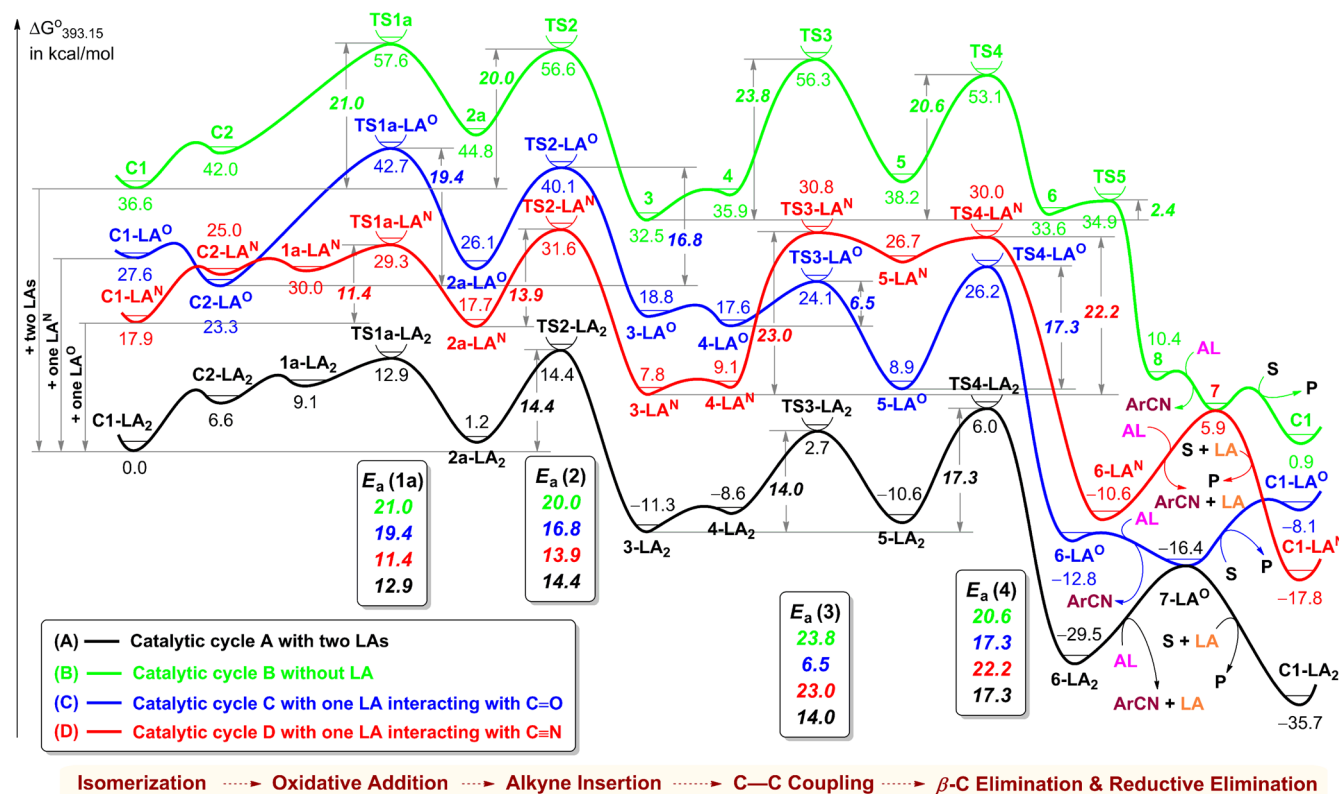


Figure 1. Gibbs energy profiles ($\Delta G^\circ_{393.15}$) of the catalytic reaction in cases A–D. In case A, two LAs interact with substrate S. In case B, no LA interacts with the substrate. In case C, one LA interacts with the carbonyl oxygen atom of the substrate. In case D, one LA interacts with the cyano nitrogen atom of the substrate.

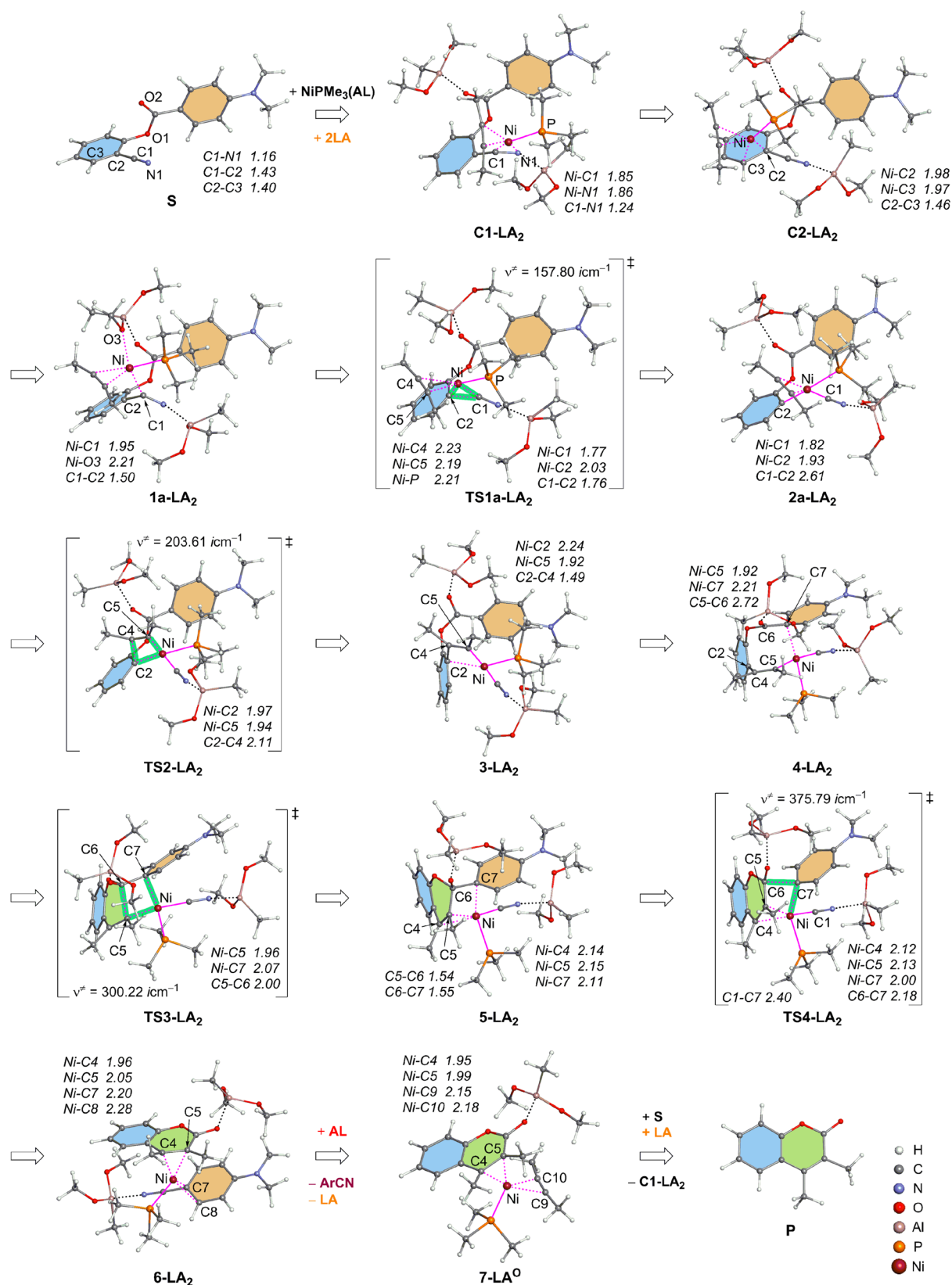
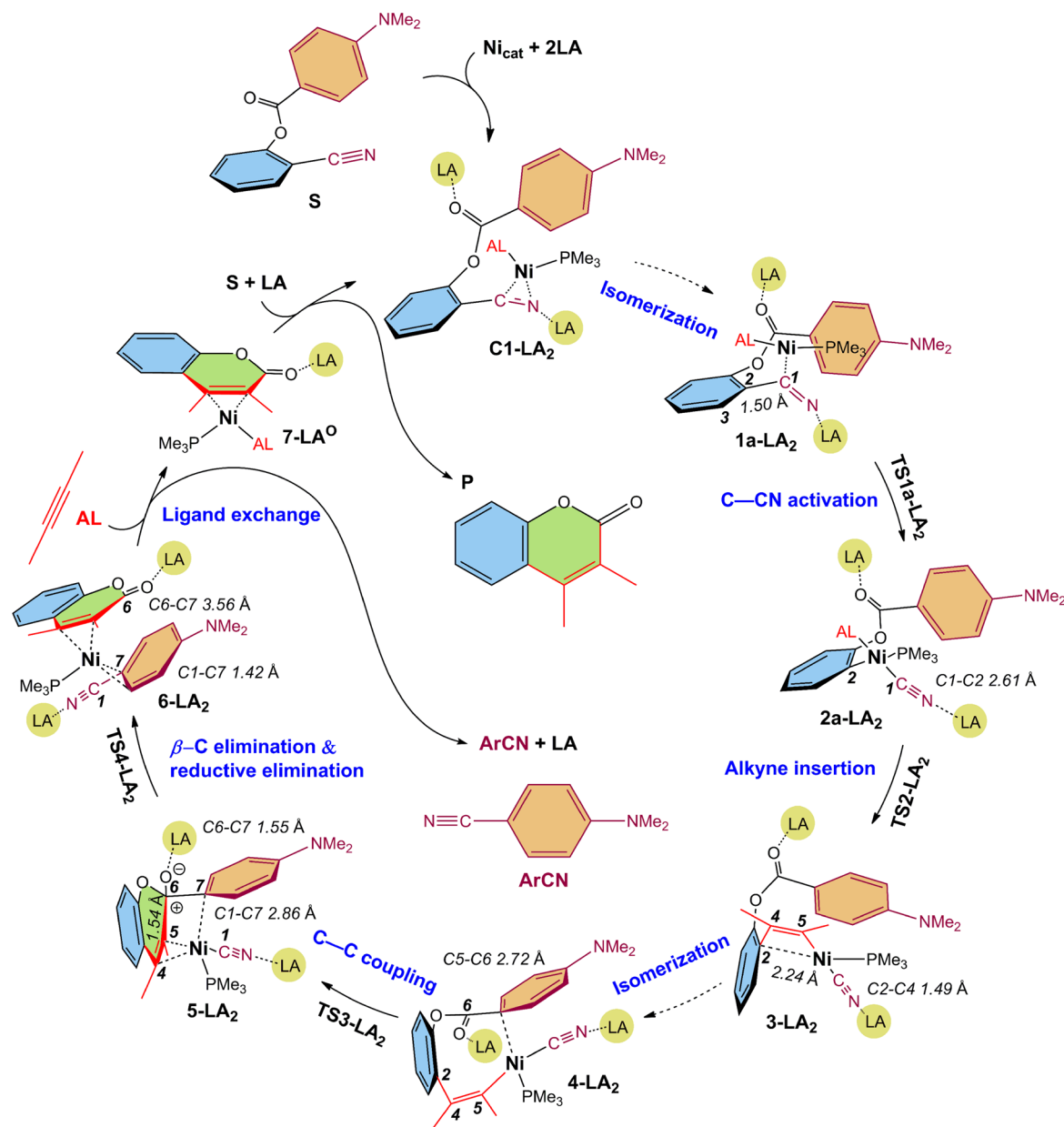


Figure 2. Geometry changes in the reaction when two LAs are present (case A). The bond distances are given in angstroms and bond angles in degrees.

of the benchmark calculations in our previous study of nickel(0)-catalyzed reactions.³¹ The solvent effect of toluene was evaluated by the conductor-like polarizable continuum model (CPCM).³² Two kinds of basis set systems were employed here. In basis set

system I (BS-I), the Los Alamos relativistic effective core potentials (ECPs)³³ were used for the core electrons of Ni and a (541/541/311/1) basis set^{33–35} was employed for its valence electrons. The 6-31G(d) basis sets were employed for other

Scheme 2. Full Catalytic Cycle in the Presence of Two LA Molecules



main-group elements. A better basis set system (BS-II) was used to evaluate the potential energy changes. In BS-II, a (311111/22111/411/11) basis set^{36,37} was employed for Ni with the ECPs of the Stuttgart–Dresden–Bonn group.³⁶ The 6-311+G(2d,p) basis sets were used for other elements. Thermal corrections and entropy contributions of vibrational movements to the Gibbs energy change were evaluated at the M06/BS-I level at 393.15 K and 1 atm, where the solvation effect was incorporated with the CPCM model due to its important influence on the activation energy of the catalytic reaction (see Table S1 in the Supporting Information). The translational entropy was corrected with the method developed by Whitesides et al.;³⁸ see page S2 in the Supporting Information for the details. The present results are discussed on the basis of the Gibbs energy calculated on the singlet potential energy surface, because the triplet surface lies much higher than the singlet by at least 33 kcal/mol³¹ (see Table S2 in the Supporting Information). All these calculations were carried out with the Gaussian 09 program.³⁹

PMe_3 was employed as a ligand in calculations here, because PMe_3 , PPh_3 , PCy_3 , and $\text{P}(\text{CH}_2\text{Ph})_3$ were used as phosphine ligands in experiments,^{18,19} as shown in Scheme 1. 4-Dimethylamino-substituted *o*-phenylcarboxybenzonitrile (**S**) and but-2-yne (**AL**) were employed as substrates in the calculations, as in the experiments. MAD was simplified to $\text{AlMe}(\text{OMe})_2$ (**LA**).

RESULTS AND DISCUSSION

Overview of Catalytic Cycle. First, we wish to briefly discuss what elementary steps are involved in the catalytic cycle, prior to a detailed discussion about the important steps.

The experimental report indicated that the yields of the product change little at phosphine to $\text{Ni}(\text{COD})_2$ mole ratios between 1 and 2.¹⁸ Also, our recent theoretical study³¹ displayed that $\text{Ni}(\text{PMe}_3)(\text{AL})$ (Ni_{cat}) is formed as an active species even when phosphine is added to the reaction system in an amount of 2 molar equiv with respect to Ni^0 . On the basis of these results,

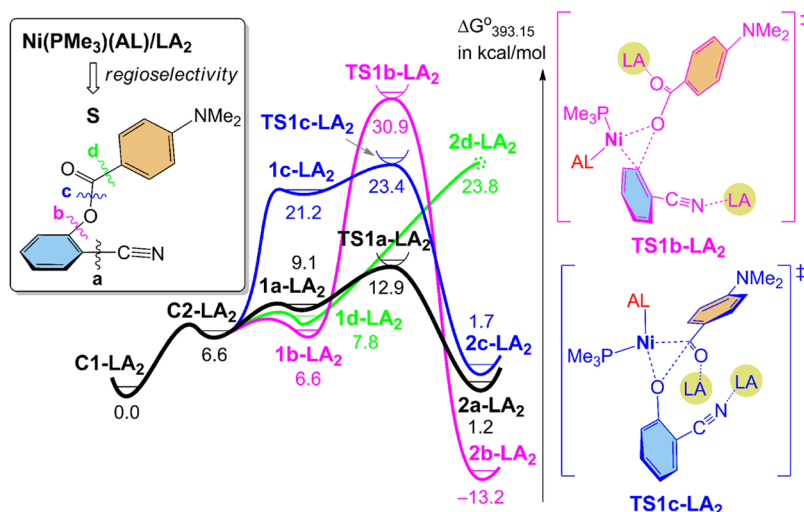


Figure 3. Gibbs energy profiles ($\Delta G^{\circ}_{393.15}$) of oxidative activation. **2d-LA₂** could be optimized by assuming the d bond distance to be 2.39 Å, which is a reasonable value.

Ni_{cat} is employed here as an active species of this catalytic reaction.

We systematically investigated four cases of the Ni^0/LA_n -catalyzed [4 + 2] cycloaddition of *o*-phenylcarboxybenzonitrile (**S**) with but-2-yne (**AL**), where *n* is 0–2. In case **A**, two **LA**s interact with the carbonyl oxygen and the cyano nitrogen atoms of **C1**, where $\text{Ni}(\text{PMe}_3)(\text{AL})(\text{S})(\text{LA})_2$ is denoted **C1-LA₂** hereafter. In case **B**, no **LA** participates in the reaction. In case **C**, one **LA** interacts with the carbonyl oxygen atom of **C1**, where $\text{Ni}(\text{PMe}_3)(\text{AL})(\text{S})(\text{LA on O})$ is denoted **C1-LA^O**. In case **D**, one **LA** interacts with the cyano nitrogen atom of **C1**, where $\text{Ni}(\text{PMe}_3)(\text{AL})(\text{S})(\text{LA on N})$ is denoted **C1-LA^N**.

The Gibbs energy profiles in Figure 1 clearly show that case **A** is the most favorable, where **C1-LA₂** is taken as a standard (energy 0); see Figure 2 for the geometry changes. As presented in Scheme 2, the catalytic cycle consists of five key elementary steps: oxidative addition of the C–CN σ -bond of **S** to the nickel(0) center (the first C–C σ -bond cleavage) to afford the nickel(II) aryl cyanide intermediate **2a-LA₂**, alkyne insertion into the nickel–aryl bond to form the nickel(II) vinyl cyanide intermediate **3-LA₂** followed by isomerization to **4-LA₂**, C–C coupling (ring closing) between the vinyl carbon and the acyl carbon atoms to afford the nickel(II) complex of coumarin derivative **5-LA₂**, β -aryl elimination (the second C–C σ -bond cleavage), and reductive elimination of coumarin (**P**) to afford the nickel(0) coumarin complex **6-LA₂**. The rate-determining step is the β -aryl elimination, the Gibbs activation energy ($\Delta G^{\circ\ddagger}$) of which is moderate (17.3 kcal/mol), as shown in Figure 1.

When **LA** is absent in the catalytic reaction (case **B**), $\text{Ni}(\text{PMe}_3)(\text{AL})(\text{S})$ **C1** without **LA** is a starting compound. **C1** is less stable than **C1-LA₂** by 36.6 kcal/mol, as shown in Figure 1 (green line), indicating that the coordination of two **LA**s with **C1** easily occurs when 2 molar equiv of **LA** is added to a nickel(0) complex. The rate-determining step is the C–C coupling (**3** → **4** → **5**), the $\Delta G^{\circ\ddagger}$ value of which is 23.8 kcal/mol; see the green line in Figure 1 and Figure S1 in the Supporting Information for the geometry changes. When only one **LA** interacts with the carbonyl oxygen atom (case **C**), $\text{Ni}(\text{PMe}_3)(\text{AL})(\text{S})(\text{LA on O})$ (**C1-LA^O**) is a starting compound. This is less stable than **C1-LA₂** by 27.6 kcal/mol, as shown in Figure 1 (blue line), indicating that **LA** strongly interacts with the carbonyl oxygen atom when **LA** is present in the reaction system. The rate-determining step is

the oxidative addition of the C–CN σ -bond to the nickel center (**C2-LA^O** → **2a-LA^O**), the $\Delta G^{\circ\ddagger}$ value of which is 19.4 kcal/mol; see the blue line in Figure 1 and Figure S2 (Supporting Information) for geometry changes. When one **LA** interacts with the cyano nitrogen atom (case **D**), $\text{Ni}(\text{PMe}_3)(\text{AL})(\text{S})(\text{LA on N})$ (**C1-LA^N**) is a starting compound. **C1-LA^N** is less stable than **C1-LA₂** by 17.9 kcal/mol, as shown in Figure 1 (a red line), indicating that **LA** also strongly interacts with the cyano nitrogen atom when **LA** is present in the reaction system. The rate-determining step is C–C coupling followed by β -aryl elimination, the $\Delta G^{\circ\ddagger}$ value of which is 23.0 kcal/mol; see the red line in Figure 1 and Figure S3 (Supporting Information) for geometry changes. These results lead us to the following clear conclusions: (i) when **LA** is added to the reaction system, **LA** strongly interacts with the carbonyl oxygen and cyano nitrogen atoms, (ii) in case **A** with two **LA** molecules, the catalytic reaction easily occurs with a moderate $\Delta G^{\circ\ddagger}$ value, while the catalytic reaction is difficult in cases **B–D**, in which either no **LA** or one **LA** is added to the reaction system, and (iii) the presence of two **LA** molecules in the reaction system is crucial for the activation of two nonstrained C–C σ -bonds. These conclusions are consistent with the experimental results¹⁸ that 3 molar equiv of **LA** molecules must be added to the nickel(0) complex.⁴⁰

Oxidative Addition of the C–CN σ -Bond to the Nickel(0) Center. The first important elementary step is the oxidative addition of the C–CN σ -bond of the substrate **S** to the nickel(0) center. This is the first C–C σ -bond cleavage. As shown in Figure 2, the $\text{C}\equiv\text{N}$ triple bond of **S** coordinates with the catalyst Ni_{cat} in a η^2 -side-on manner to form the nickel(0) complex $\text{Ni}(\text{PMe}_3)(\text{AL})(\text{S})$ (**C1-LA₂**). In this complex, two **LA**s interact with **S** through the cyano nitrogen and the carbonyl oxygen atoms, because the cyano nitrogen and carbonyl oxygen atoms have a lone pair orbital; see Figure S4 for the electrostatic potential of **S** and a discussion in the Supporting Information. Prior to the oxidative addition, the nickel(0) center approaches the C–CN σ -bond to afford the intermediate **1a-LA₂** through the η^2 -aryl-coordinated intermediate **C2-LA₂** (Figure 2). This isomerization occurs with a $\Delta G^{\circ\ddagger}$ value of 9.1 kcal/mol (Figure 1A). A similar isomerization was reported in theoretical studies of the oxidative addition of phenyl chloride⁴¹ and benzonitrile^{22e,g,41a} to nickel(0) complexes.

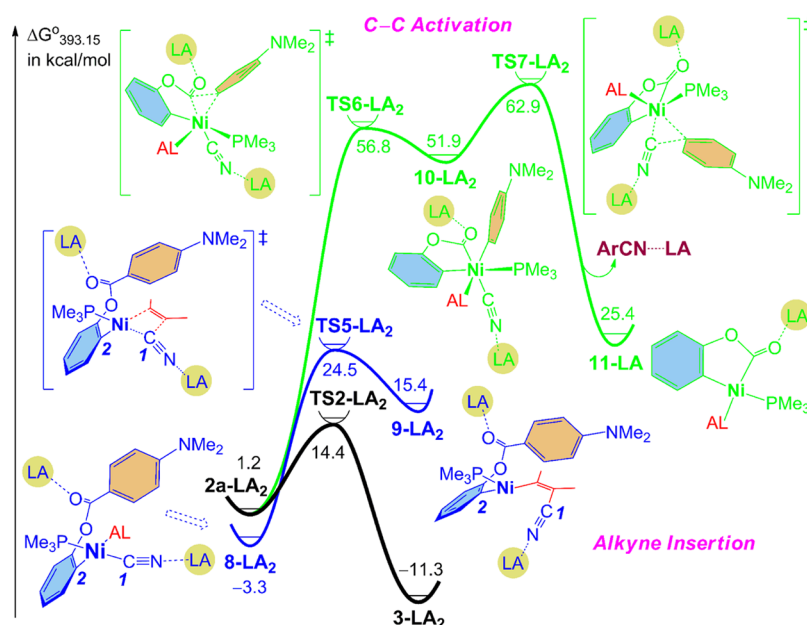


Figure 4. Gibbs energy profiles ($\Delta G^{\circ}_{393.15}$) of alkyne insertion and aryl-carbonyl bond activation.

In the oxidative addition of **S** to the nickel(0) center, we need to investigate which of four σ -bonds (a–d) of **S** undergoes the activation; see the inset in Figure 3 for bonds a–d. This selectivity is important because the reaction product depends on which bond is cleaved. From bond energy calculations on the substrates **S** and **S-LA₂**, it can be determined that the bond energy (in kcal/mol) changes in the order a (138.5) > d (121.1) > b (107.4) > c (89.3) for **S** and d (147.4) > a (133.5) > b (110.4) > c (102.4) for **S-LA₂**. It seems that activation of bond c (C=O)–O σ -bond) is the most favorable. However, kinetic calculations give different results for four σ -bond activation reactions in **S-LA₂**, because charge transfer from **Ni_{cat}** to the lowest unoccupied molecular orbital (LUMO) of **S-LA₂** leads to weakening of the a bond (C–CN σ -bond), which determines the regioselectivity of the oxidative addition;³¹ see Figure S5 in the Supporting Information for the LUMOs of **S** and **S-LA₂**. As shown in Figure 3, the a bond is cleaved via the transition state **TS1a-LA₂** with the smallest ΔG^{\ddagger} value (12.9 kcal/mol), whereas the oxidative additions of the b and c bonds (via **TS1b-LA₂** and **TS1c-LA₂**) require much larger ΔG^{\ddagger} values (30.9 and 23.4 kcal/mol, respectively). In addition, the product of the oxidative addition of the d bond could not be located.⁴² On the basis of these results, it is concluded that the first step is the oxidative addition of the C–CN σ -bond to **Ni_{cat}**.

Alkyne (AL) Insertion into the Nickel(II)–Aryl Bond.

After oxidative addition, two reaction courses such as the insertion of **AL** into the Ni(II)–C bond and the activation of the second C–C (aryl-carbonyl) σ -bond are plausible candidates. In the alkyne insertion starting from **2a-LA₂**, two reaction routes are possible; in one, **AL** is inserted into the nickel(II)–aryl (Ni–C2) bond and in the other into the nickel(II)–cyanide (Ni–C1) bond. As shown in Figure 4, the former reaction (**2a-LA₂** → **TS2-LA₂** → **3-LA₂**) occurs more easily with a moderate ΔG^{\ddagger} value (14.4 kcal/mol relative to **C1-LA₂**) in comparison to the latter reaction (**8-LA₂** → **TS5-LA₂** → **9-LA₂**), which needs a large ΔG^{\ddagger} value (27.8 kcal/mol relative to **8-LA₂**) and a positive ΔG° value of 18.7 kcal/mol. In the transition state **TS2-LA₂**, C4 is approaching C2 and an approximately planar four-membered ring (Ni–C2–C4–C5) is formed, as shown in Figure 2. In the

insertion product **3-LA₂**, a nickel(II)–aryl bonding interaction is formed between the π orbital of the aryl group and the empty d orbital of the nickel(II) center; see the Ni–C2 distance of 2.24 Å.

On the other hand, the second C–C σ -bond cleavage is very difficult; as shown in Figure 4, it occurs through the transition state **TS6-LA₂** to afford the six-coordinate Ni(IV) intermediate **10-LA₂** with a very large ΔG^{\ddagger} value (56.8 kcal/mol relative to **C1-LA₂**) and a very positive ΔG° value (50.7 kcal/mol). This result is not surprising because the nickel(IV) species is not very stable in general. Then, Ar–CN reductive elimination occurs through the transition state **TS7-LA₂** to form the four-coordinate Ni(II) intermediate **11-LA**. This reductive elimination also needs a very large ΔG^{\ddagger} value (62.9 kcal/mol relative to **C1-LA₂**). Hence, it is concluded that the second step is not the second C–C σ -bond cleavage but the alkyne insertion into the nickel–aryl (Ni–C2) bond.

At the end of this section, we wish to mention the regioselectivity in the insertion of unsymmetrical alkynes into the Ni–Ph bond, because several unsymmetrical alkenes were employed in the experiment.¹⁸ The regioselectivity in the alkyne insertion into the Ni–acyl bond was investigated in our recent theoretical study.³¹ The calculated results indicated that both electronic and steric factors influence the regioselectivity of alkyne insertion but the latter factors play a major role.³¹ This explanation is also useful to understand the regioselectivity of the present insertion reaction; see page S10 in the Supporting Information for a more detailed explanation.

C–C Coupling between the Vinyl Carbon and Carbonyl Carbon Atoms.

Because the second C–C σ -bond cleavage is not easy, some other transformation must occur before it. In **3-LA₂**, the phenyl moiety does not interact with the nickel center; see Figure 2 and Scheme 2. Because the phenyl group has π -electrons which are useful for making a bonding interaction with the nickel(II) center, it is likely that this phenyl group changes its position so as to form a bonding interaction with the nickel(II) center. As presented in Scheme 2 and Figure 2, such isomerization of **3-LA₂** occurs with a very small ΔG^{\ddagger} value of 2.7 kcal/mol to afford the eight-membered-ring intermediate **4-**

LA_2 . In 4-LA_2 , the phenyl carbon certainly interacts with the nickel(II) center; see Figure 2.

Because the carbonyl carbon (C6) is electron deficient and the vinyl carbon (C5) is electron rich, the C–C coupling reaction occurs between the C5 and C6 atoms starting from 4-LA_2 to afford the intermediate 5-LA_2 through the transition state TS3-LA_2 . In TS3-LA_2 , C6 approaches C5 but the Ni–C5 and Ni–C7 bonds are retained (Figure 2). In 5-LA_2 , a new six-membered ring (shown in green) including a $-\text{O}-\text{C6}(=\text{O})-$ group is formed and its C4–C5 double bond coordinates with the nickel(II) center; see Figure 2 and Scheme 2. In this intermediate, a coumarin structure has been almost formed. The ΔG^{\ddagger} and ΔG° values relative to 3-LA_2 are 14.0 and 0.7 kcal/mol, respectively, indicating that this process occurs easily.

β -Aryl Elimination (Second C–C σ -Bond Cleavage) Followed by Reductive Elimination. In 5-LA_2 , the C6–C7 bond becomes weak in comparison to that in 4-LA_2 , because the C7 atom interacts with the nickel(II) center and the C6 atom forms a covalent bond with the C5 atom. Actually, the C6–C7 bond cleavage occurs concomitantly with the strengthening of the Ni–C7 bonding interaction through the transition state TS4-LA_2 , as shown in Figure 2. Simultaneously, the conjugation in the six-membered ring including the $-\text{O}-\text{C6}(=\text{O})-\text{C5}-$ moiety becomes stronger as the C6–C7 bond cleavage proceeds. These geometrical changes indicate that this step is understood to be β -aryl elimination. Note that the oxidative addition of the C6–C7 bond is difficult because 5-LA_2 is a nickel(II) complex. Though one could expect that β -aryl elimination leads to the formation of a nickel(II) coumarin aryl cyanide complex, this complex could not be optimized here; rather, the nickel(0) coumarin 4-dimethylaminobenzonitrile complex 6-LA_2 was optimized, as shown in Figure 2 and Scheme 2. These geometry changes indicate that the β -aryl elimination occurs concomitantly with the reductive elimination of the Ar–CN bond in one step. In the transition state TS4-LA_2 (Figure 2), the C6–C7 distance is considerably elongated to 2.18 Å but the C1–C7 distance is still long (2.40 Å), indicating that the C6–C7 bond cleavage is the origin of the activation barrier. In 6-LA_2 , the C6–C7 bond is completely cleaved and the C1–C7 bond (1.42 Å) is formed (Figure 2). The ΔG^{\ddagger} and ΔG° values relative to 5-LA_2 are 16.6 and -18.9 kcal/mol, respectively, indicating that this process occurs easily.

Finally, the desired product coumarin **P** is released with the byproduct 4-dimethylaminobenzonitrile through ligand exchange to regenerate C1-LA_2 . In case A, the rate-determining step is β -aryl elimination followed by reductive elimination, as shown in Figure 1 (the black line). The ΔG^{\ddagger} value for the overall catalytic cycle corresponds to the energy difference between TS4-LA_2 and 3-LA_2 , because 3-LA_2 is the most stable intermediate before the most unstable transition state, TS4-LA_2 . This value is 17.3 kcal/mol, and the total ΔG° value is -35.7 kcal/mol. This calculated ΔG^{\ddagger} value seems to be lower than the expectation from the given experimental conditions (120 °C). Three reasons would be plausible; in one, the conversion of $\text{Ni}(\text{cod})_2$ to an active species needs an unexpectedly large ΔG^{\ddagger} value, and in the second, the smaller LA employed in the calculation in comparison to methylaluminum bis(2,6-di-*tert*-butyl-4-methylphenoxide) (MAD) employed in experiments^{18,19} leads to a smaller than expected ΔG^{\ddagger} value. The third reason is the concentration of the Lewis acid; 3 molar equiv of the Lewis acid is added to the solution of the Ni complex, indicating that the Lewis acid interacts with both the substrate coordinating to the Ni center and the free substrate. This means

that the substrate coordinated with the Ni center does not find enough free Lewis acid and thereby the reaction must occur without two Lewis acid molecules.

Roles of Lewis Acids in Each Elementary Step. In this catalytic reaction via dual C–C σ -bond activations, the presence of excess Lewis acid (MAD) is crucial because no product or very little product is produced in the absence of LA.¹⁸ In this regard, systematic assessment of the effects of LA is of considerable importance to understand well this catalytic reaction and elucidate the reasons two nonstrained C–C σ -bonds are successfully cleaved by the Ni^0/LA system. For this purpose, we investigated the reaction without LA (case B), the reaction with one LA on the carbonyl oxygen atom (case C), and the reaction with one LA on the cyano nitrogen (case D), as mentioned above. Here, we wish to discuss the effects of LA in each elementary step.

In the C–CN σ -bond activation via oxidative addition, the ΔG^{\ddagger} value is 12.9 kcal/mol in case A (the bottom black line in Figure 1), 21.0 kcal/mol in case B (the top green line), 19.4 kcal/mol in case C (the middle blue line), and 11.4 kcal/mol in case D (the middle red line). These results clearly show that one LA coordinated with the cyano nitrogen atom (named LA^{N}) dramatically accelerates the C–CN σ -bond cleavage.

In the alkyne insertion, the ΔG^{\ddagger} value is 13.2 kcal/mol (relative to the intermediate 2a-LA_2) in case A, 11.8 kcal/mol relative to 2a in case B, 14.0 kcal/mol relative to 2a-LA^{O} in case C, and 13.9 kcal/mol relative to 2a-LA^{N} in case D. Thus, it should be concluded that the presence of LA interacting with the cyano nitrogen and carbonyl oxygen atoms does not influence the alkyne insertion very much.

In the C–C coupling step, the ΔG^{\ddagger} is 14.0 kcal/mol relative to 3-LA_2 in case A, 23.8 kcal/mol relative to 3 in case B, 6.5 kcal/mol relative to 4-LA^{O} in case C, and 23.0 kcal/mol relative to 3-LA^{N} in case D. The ΔG° values for this process are 0.7 kcal/mol in case A, 5.7 kcal/mol in case B, -9.9 kcal/mol in case C, and 18.9 kcal/mol in case D. On the basis of these results, it is concluded that the LA interacting with the carbonyl oxygen atom (named LA^{O}) effectively decreases the activation barrier and the reaction energy in the C–C coupling but LA^{N} suppresses the C–C coupling.

For the β -aryl elimination (the second C–C σ -bond activation), the ΔG^{\ddagger} value is 16.6 kcal/mol relative to 5-LA_2 in case A, 14.9 kcal/mol relative to 5 in case B, 17.3 kcal/mol relative to 5-LA^{O} in case C, and 3.3 kcal/mol relative to 5-LA^{N} in case D. These results indicate that LA^{O} suppresses the β -aryl elimination but LA^{N} accelerates it. Though the ΔG^{\ddagger} value for the β -aryl elimination is very small in case D, it should be noted that this very small ΔG^{\ddagger} value arises from the very unstable 5-LA^{N} , as shown in Figure 1. Because TS4-LA^{N} is as unstable as TS3-LA^{N} , the energy barrier for the β -aryl elimination relative to the stable intermediate 3-LA^{N} is as large as the barrier for the C–C coupling in case D.

What is important is not the ΔG^{\ddagger} value for the β -aryl elimination but the ΔG^{\ddagger} value to reach the intermediate 6-LA_2 , 6-LA^{O} , 6-LA^{N} , or 6 from the stable intermediate 3-LA_2 , 3-LA^{O} , 3-LA^{N} , or 3 , respectively; see Figure 1. These ΔG^{\ddagger} values are 17.3 kcal/mol, which is the energy difference between TS4-LA_2 and 3-LA_2 in case A, 23.8 kcal/mol, which is the energy difference between TS3 and 3 in case B, 17.3 kcal/mol, which is the energy difference between TS4-LA^{O} and 5-LA^{O} in case C, and 23.0 kcal/mol, which is the energy difference between TS3-LA^{N} and 3-LA^{N} in case D; note that TS3 and TS3-LA^{N} are higher in energy than TS4 and TS4-LA^{N} , respectively, in cases B and D. In cases B and

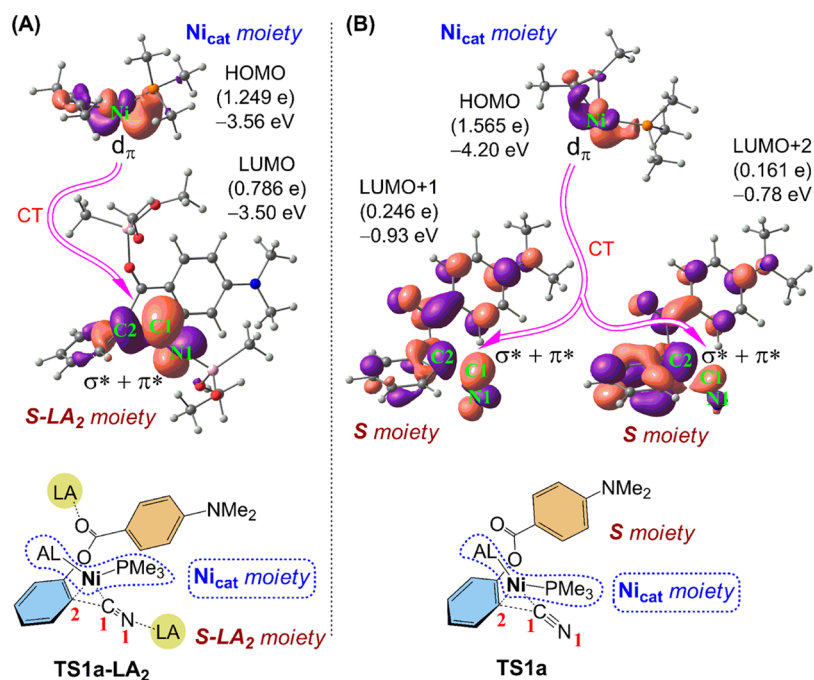


Figure 5. Important Kohn–Sham orbitals and their electron populations of Ni_{cat} and S-LA_2 (or S) moieties in TS1a-LA_2 (or TS1a).

D, the ΔG^{\ddagger} value is large because the C–C coupling is difficult due to the absence of LA^{O} . In cases **A** and **C**, the ΔG^{\ddagger} value for the β -aryl elimination is somewhat larger than that for the C–C coupling because the intermediates 5-LA_2 and 5-LA^{O} are stable but considerably smaller than those for the C–C coupling in cases **B** and **D**. On the basis of these results, it is concluded that LA^{O} is indispensable to reach the intermediate 6-LA_2 or 6-LA^{O} from 3-LA_2 and 3-LA^{O} , respectively; if LA^{O} is absent, the C–C coupling becomes very difficult and the large ΔG^{\ddagger} value is necessary to reach **6** and 6-LA^{N} . If LA^{O} is present, the C–C coupling easily occurs to afford the stable intermediates 5-LA_2 and 5-LA^{O} . The formations of the stable 5-LA_2 and 5-LA^{O} lead to the presence of lower energy TS4-LA_2 and TS4-LA^{O} , even though the ΔG^{\ddagger} value is large for the β -aryl elimination. Hence, LA^{O} is indispensable to pass through the C–C coupling and the next β -aryl elimination.

Electronic Processes of Important Elementary Steps.

To understand well the reasons why LA^{N} accelerates the C–CN σ -bond activation, we investigated the electronic process of this step with a fragment molecular orbital analysis;⁴³ see page S11 in the Supporting Information for details of the analysis. As shown in Figure 5A, TS1a-LA_2 is divided into two fragments as S-LA_2 and Ni_{cat} moieties. The electron population of the LUMO of the S-LA_2 moiety extremely increases to 0.786e in TS1a-LA_2 . Consistent with this increase in population, the population of the highest occupied molecular orbital (HOMO) of the Ni_{cat} moiety considerably decreases to 1.249e. These results clearly indicate that substantial charge transfer (CT) occurs from the HOMO of Ni_{cat} to the LUMO of S-LA_2 in the oxidative addition. The HOMO of Ni_{cat} mainly consists of the nickel $3d_{\pi}$ orbital. The LUMO of S-LA_2 in the transition state mainly consists of the σ^* orbital of the C–CN bond and the π^* orbital of the CN moiety. This LUMO is formed by $\sigma^*-\pi^*$ orbital mixing which is induced by the distorted geometry of the transition state. Because the LUMO is antibonding between the Ar and CN groups, CT to the LUMO plays an important role in the Ar–CN bond breaking.^{22f,41a} As shown in Figure 5B, TS1a without LA is divided into

S and Ni_{cat} moieties in the same way. The LUMO+1 and LUMO+2 populations of the S moiety moderately increase to 0.246e and 0.161e, respectively, in TS1a , and the population of the HOMO of the Ni_{cat} moiety correspondingly decreases to 1.565e. This means that a CT similar to that in TS1a-LA_2 from $3d_{\pi}$ to $\sigma^* + \pi^*$ is formed in TS1a . However, this CT is considerably weaker in TS1a than in TS1a-LA_2 . This is because the unoccupied $\sigma^* + \pi^*$ C–CN antibonding orbital is considerably stabilized by the interaction of LA^{N} with the cyano nitrogen atom, as follows: the unoccupied $\sigma^* + \pi^*$ C–CN orbital exists as the LUMO at -3.50 eV in TS1a-LA_2 but as the LUMO+1 and LUMO+2 at -0.93 and -0.78 eV in TS1a . These results clearly indicate that LA^{N} stabilizes the $\sigma^* + \pi^*$ C–CN antibonding orbital to enhance the CT from the $3d_{\pi}$ to the $\sigma^* + \pi^*$ and accordingly accelerate the oxidative addition. This is the first theoretical explanation for the effect of the Lewis acid on the C–CN σ -bond activation reported by Jones et al.¹⁴ and Nakao et al.¹⁵

We also found the largest difference in the ΔG^{\ddagger} value between the reactions with and without LA in the C–C coupling step. In this step, the vinyl C5 attacks the carbonyl C6 atom to form a C–C σ -bond. This step is understood to be a nucleophilic attack of C5 at C6, because the vinyl C5 is negatively charged but the carbonyl C6 is positively charged. LA^{O} stabilizes the LUMO of the carbonyl by interacting with the carbonyl oxygen atom to enhance the electrophilic feature of the C5 atom and accelerate the C5–C6 coupling via nucleophilic attack. This is also favorable for the second C–C σ -bond cleavage via the β -aryl elimination, because 5-LA_2 and TS4-LA_2 are stabilized by the interaction of LA^{O} with the carbonyl oxygen atom, as was discussed above.

CONCLUSIONS

Nickel(0)/ LA -catalyzed decyanative [4 + 2] cycloaddition of *o*-arylcyanobenzonitrile with alkyne was systematically investigated with the DFT method. The theoretical calculations clearly disclose the mechanistic details, the origins of cooperative catalysis of the nickel(0)/ LA system, and the reasons two

nonstrained C–C σ -bonds are successfully cleaved by the presence of two LA molecules.

The catalytic cycle consists of oxidative addition of the C–CN σ -bond to the nickel(0) center, alkyne insertion into the nickel(II)–aryl bond, C–C coupling between the vinyl carbon and carboxyl carbon atoms, and β -aryl elimination followed by reductive elimination. Under the most favorable reaction conditions with two LA molecules, the rate-determining step is β -aryl elimination followed by reductive elimination, the ΔG^{\ddagger} value of which is moderate (17.3 kcal/mol). One LA interacting with the cyano nitrogen atom of **S** dramatically promotes the C–CN σ -bond activation by stabilizing the unoccupied $\sigma^* + \pi^*$ C–CN antibonding orbital. One more LA interacting with the carbonyl oxygen of **S** effectively accelerates the C–C coupling followed by β -aryl elimination. This acceleration is achieved because LA on the carbonyl oxygen atom increases the electrophilic nature of the carboxyl carbon. If only one LA interacts with the cyano nitrogen atom, the C–CN σ -bond activation is accelerated but the C–C coupling becomes difficult. If only one LA interacts with the carbonyl oxygen atom, the C–C coupling is accelerated but the C–CN σ -bond cleavage becomes difficult. Hence, the presence of two LA molecules is crucial to perform this catalytic reaction. These results are consistent with the experimental results.¹⁸

The above understanding provides new ideas on how to cleave two nonstrained C–C σ -bonds by the presence of a Lewis acid molecule; the oxidative addition of the C–CN σ -bond of nitrile to a low-valent TM complex is greatly accelerated by one Lewis acid interacting with the cyano nitrogen atom because the LA stabilizes the $\sigma^* + \pi^*$ antibonding orbital of the C–CN bond. The β -aryl elimination of aryl-COR occurs easily after the C–C bond formation between the carbonyl carbon of the COR group and some other carbon atoms, because such C–C bond formation weakens the C–C bond between the aryl and COR groups. A Lewis acid interacting with the carbonyl oxygen atom accelerates the C–C coupling and the β -aryl elimination by stabilizing the intermediate and transition state. This LA-assisted C–C σ -bond cleavage via β -aryl elimination is first recognized here as an important C–C σ -bond activation reaction. At the end of this section, we wish to mention the possibility that the reaction can occur without the Lewis acid because the ΔG^{\ddagger} value is 23.8 kcal/mol even without the Lewis acid if we can select a favorable substrate and alkyne. Such an experiment is challenging.

■ ASSOCIATED CONTENT

Supporting Information

The following file is available free of charge on the ACS Publications website at DOI: 10.1021/cs501653s.

Correction of translational entropy, FMO analysis method, Figures S1–S5, Tables S1–S3, and Cartesian coordinates of optimized structures in this work ([PDF](#))

■ AUTHOR INFORMATION

Corresponding Author

*E-mail for S.S.: sakaki.shigeyoshi.47e@st.kyoto-u.ac.jp.

Notes

The authors declare no competing financial interest.

■ ACKNOWLEDGMENTS

This work has been financially supported by the Ministry of Education, Culture, Science, Sport, and Technology through a

Grant-in-Aid of Specially Promoted Science and Technology (no. 22000009). W.G. is also grateful to the National Science Fund in China (21403033). We wish to thank the computer center of the Institute for Molecular Science (IMS, Okazaki, Japan) for the kind use of their computers.

■ REFERENCES

- (1) See recent review articles: (a) van der Boom, M. E.; Milstein, D. *Chem. Rev.* **2003**, *103*, 1759–1792. (b) Jun, C.-H. *Chem. Soc. Rev.* **2004**, *33*, 610–618. (c) Tobisu, M.; Chatani, N. *Chem. Soc. Rev.* **2008**, *37*, 300–307. (d) Bonesi, S. M.; Fagnoni, M. *Chem. Eur. J.* **2010**, *16*, 13572–13589. (e) Murakami, M.; Matsuda, T. *Chem. Commun.* **2011**, *47*, 1100–1105. (f) Ruhland, K. *Eur. J. Org. Chem.* **2012**, 2683–2706.
- (2) Trost, B. M. *Science* **1991**, *254*, 1471–1477.
- (3) (a) Sakaki, S.; Ieki, M. *J. Am. Chem. Soc.* **1993**, *115*, 2373–2381. (b) Sakaki, S.; Mizoe, N.; Musashi, Y.; Sugimoto, M. *J. Phys. Chem. A* **1998**, *102*, 8027–8036. (c) Rytchinski, B.; Milstein, D. *Angew. Chem., Int. Ed.* **1999**, *38*, 870–883.
- (4) (a) Rubin, M.; Rubina, M.; Gevorgyan, V. *Chem. Rev.* **2007**, *107*, 3117–3179. (b) Matsuda, T.; Shigeno, M.; Murakami, M. *J. Am. Chem. Soc.* **2007**, *129*, 12086–12087. (c) Seiser, T.; Roth, O. A.; Cramer, N. *Angew. Chem., Int. Ed.* **2009**, *48*, 6320–6323. (d) Seiser, T.; Cramer, N. *J. Am. Chem. Soc.* **2010**, *132*, 5340–5341. (e) Lin, M.; Li, F.; Jiao, L.; Yu, Z.-X. *J. Am. Chem. Soc.* **2011**, *133*, 1690–1693. (f) Thakur, A.; Facer, M. E.; Louie, J. *Angew. Chem., Int. Ed.* **2013**, *52*, 12161–12165. (g) Masarwa, A.; Didier, D.; Zabrodski, T.; Schinkel, M.; Ackermann, L.; Marek, I. *Nature* **2014**, *505*, 199–203. (h) Chen, P.-H.; Xu, T.; Dong, G.-B. *Angew. Chem., Int. Ed.* **2014**, *53*, 1674–1678. (i) Souillart, L.; Parker, E.; Cramer, N. *Angew. Chem., Int. Ed.* **2014**, *53*, 3001–3005.
- (5) (a) Fisher, E. L.; Lampert, T. H. *Org. Lett.* **2009**, *11*, 4108–4110. (b) Youn, S. W.; Kim, B. S.; Jagdale, A. R. *J. Am. Chem. Soc.* **2012**, *134*, 11308–11311.
- (6) (a) Dreis, A. M.; Douglas, C. J. *J. Am. Chem. Soc.* **2009**, *131*, 412–413. (b) Sattler, A.; Parkin, G. *Nature* **2010**, *463*, 523–526. (c) Li, H.; Li, Y.; Zhang, X.-S.; Chen, K.; Wang, X.; Shi, Z.-J. *J. Am. Chem. Soc.* **2011**, *133*, 15244–15247.
- (7) (a) Gooßen, L. J.; Deng, G.-J.; Levy, L. M. *Science* **2006**, *313*, 662–664. (b) Cicchillo, R. M.; Zhang, H.-J.; Blodgett, J. A. V.; Whitteck, J. T.; Li, G.-Y.; Nair, S. K.; van der Donk, W. A.; Metcalf, W. W. *Nature* **2009**, *459*, 871–874. (c) Shang, R.; Fu, Y.; Li, J.-B.; Zhang, S.-L.; Guo, Q.-X.; Liu, L. *J. Am. Chem. Soc.* **2009**, *131*, 5738–5739. (d) Pusterla, I.; Bode, J. W. *Angew. Chem., Int. Ed.* **2012**, *51*, 513–516.
- (8) (a) Kajita, Y.; Kurahashi, T.; Matsubara, S. *J. Am. Chem. Soc.* **2008**, *130*, 17226–17227. (b) He, C.; Guo, S.; Huang, L.; Lei, A.-W. *J. Am. Chem. Soc.* **2010**, *132*, 8273–8275. (c) Amaike, K.; Muto, K.; Yamaguchi, J.; Itami, K. *J. Am. Chem. Soc.* **2012**, *134*, 13573–13576.
- (9) (a) Tobisu, M.; Kita, Y.; Ano, Y.; Chatani, N. *J. Am. Chem. Soc.* **2008**, *130*, 15982–15989. (b) Tobisu, M.; Kinuta, H.; Kita, Y.; Rémond, E.; Chatani, N. *J. Am. Chem. Soc.* **2012**, *134*, 115–118.
- (10) (a) Shi, Y. L.; Roth, K. E.; Ramgren, S. D.; Blum, S. A. *J. Am. Chem. Soc.* **2009**, *131*, 18022–18023. (b) Liu, X.; Henderson, J. A.; Sasaki, T.; Kishi, Y. *J. Am. Chem. Soc.* **2009**, *131*, 16678–16680. (c) Trost, B. M.; Luan, X. *J. Am. Chem. Soc.* **2011**, *133*, 1706–1709. (d) Mustard, T. J. L.; Mack, D. J.; Njardarson, J. T.; Cheong, P. H.-Y. *J. Am. Chem. Soc.* **2013**, *135*, 1471–1475.
- (11) (a) Park, Y. J.; Park, J.-W.; Jun, C.-H. *Acc. Chem. Res.* **2008**, *41*, 222–234. (b) Shao, Z.-H.; Zhang, H.-B. *Chem. Soc. Rev.* **2009**, *38*, 2745–2755. (c) Yeung, C. S.; Dong, V.-M. *Angew. Chem., Int. Ed.* **2011**, *50*, 809–812. (d) Quintard, A.; Alexakis, A.; Mazet, C. *Angew. Chem., Int. Ed.* **2011**, *50*, 2354–2358. (e) Skucas, E.; MacMillan, D. W. C. *J. Am. Chem. Soc.* **2012**, *134*, 9090–9093. (f) DiRocco, D. A.; Rovis, T. *J. Am. Chem. Soc.* **2012**, *134*, 8094–8097. (g) Krautwald, S.; Sarlah, D.; Schafroth, M. A.; Carreira, E. M. *Science* **2013**, *340*, 1065–1068.
- (12) (a) Burns, N. Z.; Written, M. R.; Jacobsen, E. N. *J. Am. Chem. Soc.* **2011**, *133*, 14578–14581. (b) Mittal, N.; Sun, D.-X.; Seidel, D. *Org. Lett.* **2012**, *14*, 3084–3087. (c) Min, C.; Mittal, N.; De, C. K.; Seidel, D. *Chem. Commun.* **2012**, *48*, 10853–10855. (d) Rueping, M.; Volla, C. M. R.; Atodiresei, I. *Org. Lett.* **2012**, *14*, 4642–4645.

- (13) Wang, C.-Y.; Xi, Z.-F. *Chem. Soc. Rev.* **2007**, *36*, 1395–1406.
- (14) Brunkan, N. M.; Brestensky, D. M.; Jones, W. D. *J. Am. Chem. Soc.* **2004**, *126*, 3627–3641.
- (15) (a) Nakao, Y.; Yada, A.; Ebata, S.; Hiyama, T. *J. Am. Chem. Soc.* **2007**, *129*, 2428–2429. (b) Nakao, Y.; Hirata, Y.; Tannaka, M.; Hiyama, T. *Angew. Chem., Int. Ed.* **2008**, *47*, 385–387. (c) Nakao, Y.; Ebata, S.; Yada, A.; Hiyama, T.; Ikawa, M.; Ogoshi, S. *J. Am. Chem. Soc.* **2008**, *130*, 12874–12875. (d) Nakao, Y.; Yada, A.; Hiyama, T. *J. Am. Chem. Soc.* **2010**, *132*, 10024–10026. (e) Hirata, Y.; Yada, A.; Morita, E.; Nakao, Y.; Hiyama, T.; Ohashi, M.; Ogoshi, S. *J. Am. Chem. Soc.* **2010**, *132*, 10070–10077. (f) Minami, Y.; Yoshiyasu, H.; Nakao, Y.; Hiyama, T. *Angew. Chem., Int. Ed.* **2013**, *52*, 883–887.
- (16) Watson, M. P.; Jacobsen, E. N. *J. Am. Chem. Soc.* **2008**, *130*, 12594–12595.
- (17) Nájera, C.; Sansano, J. M. *Angew. Chem., Int. Ed.* **2009**, *48*, 2452–2456.
- (18) Nakai, K.; Kurahashi, T.; Matsubara, S. *J. Am. Chem. Soc.* **2011**, *133*, 11066–11068.
- (19) Nakai, K.; Kurahashi, T.; Matsubara, S. *Org. Lett.* **2013**, *15*, 856–859.
- (20) (a) Nakazawa, H.; Kawasaki, T.; Miyoshi, K.; Suresh, C. H.; Koga, N. *Organometallics* **2004**, *23*, 117–126. (b) Nakazawa, H.; Kamata, K.; Itazaki, M. *Chem. Commun.* **2005**, 4004–4006.
- (21) (a) Li, X.-Y.; Sun, H.-J.; Yu, F.-L.; Flörke, U.; Klein, H.-F. *Organometallics* **2006**, *25*, 4695–4697. (b) Xu, H.-W.; Williard, P. G.; Bernskoetter, W. H. *Organometallics* **2012**, *31*, 1588–1590.
- (22) (a) Garcia, J. J.; Jones, W. D. *Organometallics* **2000**, *19*, 5544–5545. (b) Garcia, J. J.; Brunkan, N. M.; Jones, W. D. *J. Am. Chem. Soc.* **2002**, *124*, 9547–9555. (c) Garcia, J. J.; Arévalo, A.; Brunkan, N. M.; Jones, W. D. *Organometallics* **2004**, *23*, 3997–4002. (d) Ateşin, T. A.; Li, T.; Lachaize, S.; Brennessel, W. W.; Garcia, J. J.; Jones, W. D. *J. Am. Chem. Soc.* **2007**, *129*, 7562–7569. (e) Ateşin, T. A.; Li, T.; Lachaize, S.; Garcia, J. J.; Jones, W. D. *Organometallics* **2008**, *27*, 3811–3817. (f) Ohnishi, Y.-Y.; Nakao, Y.; Sato, H.; Sakaki, S. *J. Phys. Chem. A* **2007**, *111*, 7915–7924. (g) Ohnishi, Y.-Y.; Nakao, Y.; Sato, H.; Nakao, Y.; Hiyama, T.; Sakaki, S. *Organometallics* **2009**, *28*, 2583–2594.
- (23) (a) Marlin, D. S.; Olmstead, M. M.; Mascharak, P. K. *Angew. Chem., Int. Ed.* **2001**, *40*, 4752–4754. (b) Lu, T.-B.; Zhuang, X.-M.; Li, Y.-W.; Chen, S. *J. Am. Chem. Soc.* **2004**, *126*, 4760–4761.
- (24) Churchill, D.; Shin, J. H.; Hascall, T.; Hahn, J. M.; Bridgewater, B. M.; Parkin, G. *Organometallics* **1999**, *18*, 2403–2406.
- (25) Ochiai, M.; Hashimoto, H.; Tobita, H. *Angew. Chem., Int. Ed.* **2007**, *46*, 8192–8194.
- (26) (a) Taw, F. L.; White, P. S.; Bergman, R. G.; Brookhart, M. *J. Am. Chem. Soc.* **2002**, *124*, 4192–4193. (b) Taw, F. L.; Mellows, H.; White, P. S.; Hollander, F. J.; Bergman, R. G.; Brookhart, M.; Heinekey, D. M. *J. Am. Chem. Soc.* **2002**, *124*, 5100–5108. (c) Taw, F. L.; Mueller, A. H.; Bergman, R. G.; Brookhart, M. *J. Am. Chem. Soc.* **2003**, *125*, 9808–9813. (d) Evans, M. E.; Jones, W. D. *Organometallics* **2011**, *30*, 3371–3377.
- (27) Liu, Q.-X.; Xu, F.-B.; Li, Q.-S.; Song, H.-B.; Zhang, Z.-Z. *Organometallics* **2004**, *23*, 610–614.
- (28) Anand, M.; Sunoj, R. B. *Org. Lett.* **2012**, *14*, 4584–4587.
- (29) Pham, H. V.; Paton, R. S.; Ross, A. G.; Danishefsky, S. J.; Houk, K. N. *J. Am. Chem. Soc.* **2014**, *136*, 2397–2403.
- (30) Zhao, Y.; Truhlar, D. G. *Theor. Chem. Acc.* **2008**, *120*, 215–241.
- (31) Guan, W.; Sakaki, S.; Kurahashi, T.; Matsubara, S. *Organometallics* **2013**, *32*, 7564–7574.
- (32) (a) Barone, V.; Cossi, M. *J. Phys. Chem. A* **1998**, *102*, 1995. (b) Cossi, M.; Rega, N.; Scalmani, G.; Barone, V. *J. Comput. Chem.* **2003**, *24*, 669. (c) Tomasi, J.; Mennucci, B.; Cammi, R. *Chem. Rev.* **2005**, *105*, 2999–3093.
- (33) Hay, P. J.; Wadt, W. R. *J. Chem. Phys.* **1985**, *82*, 299–310.
- (34) Couty, M.; Hall, M. B. *J. Comput. Chem.* **1996**, *17*, 1359–1370.
- (35) Ehlers, A. W.; Böhme, M.; Dapprich, S.; Gobbi, A.; Höllwarth, A.; Jonas, V.; Köhler, K. F.; Stegmann, R.; Veldkamp, A.; Frenking, G. *Chem. Phys. Lett.* **1993**, *208*, 111–114.
- (36) Dolg, M.; Wedig, U.; Stoll, H.; Preuss, H. *J. Chem. Phys.* **1987**, *86*, 866–872.
- (37) Martin, J. M. L.; Sundermann, A. *J. Chem. Phys.* **2001**, *114*, 3408–3420.
- (38) Mammen, M.; Shakhnovich, E. I.; Deutch, J. M.; Whitesides, G. M. *J. Org. Chem.* **1998**, *63*, 3821–3830.
- (39) Frisch, M. J.; Trucks, G. W.; Schlegel, H. B.; Scuseria, G. E.; Robb, M. A.; Cheeseman, J. R.; Scalmani, G.; Barone, V.; Mennucci, B.; Petersson, G. A.; Nakatsuji, H.; Caricato, M.; Li, X.; Hratchian, H. P.; Izmaylov, A. F.; Bloino, J.; Zheng, G.; Sonnenberg, J. L.; Hada, M.; Ehara, M.; Toyota, K.; Fukuda, R.; Hasegawa, J.; Ishida, M.; Nakajima, T.; Honda, Y.; Kitao, O.; Nakai, H.; Vreven, T.; Montgomery, Jr., J. A.; Peralta, J. E.; Ogliaro, F.; Bearpark, M.; Heyd, J. J.; Brothers, E.; Kudin, K. N.; Staroverov, V. N.; Kobayashi, R.; Normand, J.; Raghavachari, K.; Rendell, A.; Burant, J. C.; Iyengar, S. S.; Tomasi, J.; Cossi, M.; Rega, N.; Millam, J. M.; Klene, M.; Knox, J. E.; Cross, J. B.; Bakken, V.; Adamo, C.; Jaramillo, J.; Gomperts, R.; Stratmann, R. E.; Yazyev, O.; Austin, A. J.; Cammi, R.; Pomelli, C.; Ochterski, J. W.; Martin, R. L.; Morokuma, K.; Zakrzewski, V. G.; Voth, G. A.; Salvador, P.; Dannenberg, J. J.; Dapprich, S.; Daniels, A. D.; Farkas, Ö.; Foresman, J. B.; Ortiz, J. V.; Cioslowski, J.; Fox, D. J. *Gaussian 09, Revision B.01*; Gaussian, Inc., Wallingford, CT, 2009.
- (40) A 3 molar equiv amount of LA molecules would be necessary for coordination equilibrium and interaction with free substrate.
- (41) (a) Guan, W.; Sayyed, F. B.; Zeng, G.; Sakaki, S. *Inorg. Chem.* **2014**, *33*, 6444–6457 and references therein. (b) Sayyed, F. B.; Tsuji, Y.; Sakaki, S. *Chem. Commun.* **2013**, 49, 10715–10717.
- (42) Even starting from an assumed nickel(II) intermediate **2d-LA₂** with a d bond distance of 2.39 Å, the geometry optimization leads to the stable η^2 -coordinated nickel(0) complex **1d-LA₂** (see Figure 3).
- (43) (a) Baba, H.; Suzuki, S.; Takemura, T. *J. Chem. Phys.* **1969**, *50*, 2078–2086. (b) Kato, S.; Yamabe, S.; Fukui, K. *J. Chem. Phys.* **1974**, *60*, 572–578. (c) Dapprich, S.; Frenking, G. *J. Phys. Chem.* **1995**, *99*, 9352–9362.